



# Metal-enhanced chemiluminescence detection of C-reaction protein based on silver nanoparticle hybrid probes



Chen Zong<sup>a,\*</sup>, Duoduo Zhang<sup>a,1</sup>, Fan Jiang<sup>a</sup>, Hua Yang<sup>a</sup>, Shijia Liu<sup>b</sup>, Ping Li<sup>a,\*</sup>

<sup>a</sup> State Key Laboratory of Natural Medicines, China Pharmaceutical University, Nanjing 210009, PR China

<sup>b</sup> Jiangsu Province Hospital of Traditional Chinese Medicine, Nanjing 210029, PR China

## ARTICLE INFO

### Keywords:

Metal-enhanced chemiluminescence  
Silver nanoparticle hybrid probes  
Signal amplification  
Immunosensor  
Ultrasensitive immunoassay  
Cerebrovascular disease

## ABSTRACT

A novel metal-enhanced chemiluminescence (MEC) signal tag was designed. By combining with a disposable immunosensor chip, an ultrasensitive immunoassay method was proposed for detection of C-reactive protein (CRP), an essential cerebrovascular disease marker. Two kinds of silver nanoparticle (AgNP) probes, DNA-hemin/DNA-A/biotin-DNA modified AgNPs (Probe A) and DNA-hemin/DNA-B modified AgNPs (Probe B) were prepared respectively. The MEC signal tag was formed by the link of Probe A and Probe B through the hybridization of DNA-A and DNA-B. The formed AgNP hybrid probes brought excellent CL signal amplification, due to the increased content of hemin molecules and the great MEC effect. The AgNP hybrid probes can be bound to the biotinylated antibody of sandwich immunocomplex for immunoassay of CRP. Under optimal conditions, the method showed a wide detection range of  $7 \times 10^{-7}$  to  $0.07 \text{ mg mL}^{-1}$  and a detection limit down to  $0.05 \text{ ng mL}^{-1}$ . The results obtained with clinical serum samples were in acceptable agreement with reference values. The AgNP hybrid probes as well as the MEC-based immunoassay method showed great potentials in early clinical diagnosis of cerebrovascular disease.

## 1. Introduction

Cerebrovascular diseases have endangered the health of people seriously. Early prevention and treatment of cerebrovascular disease are extremely important for improving survival rate of patients. C-reactive protein (CRP) as an acute-phase serum marker is closely related to a variety of cerebrovascular diseases, such as cerebral arterial thrombosis [1] and neurological disorders [2]. Therefore, developing an ultrasensitive, selective and accurate method for immunoassay of CRP plays a pivotal role in early screening, evaluating and monitoring of cerebrovascular disease.

In recent years, chemiluminescence (CL) becomes an effective analytical tool for detection of biomarkers [3–8]. Compared with other optical techniques, such as fluorescence spectroscopy, phosphorescence spectroscopy and ultraviolet-visible spectroscopy, CL-based detection does not require an external light source, thus reducing light scattering and eliminating undesired signal interference [9,10]. Besides, it possesses advantages of simple instrument, rapid analysis, low detection limit and wide linear range. However, CL-based detection is usually limited by the classical photochemical properties of reaction yield and quantum yield. Thus, increased quantum yield and accelerated CL

reactions are in demand to enhance the sensitivity and efficiency of CL-based bioassays [11].

Metal surface plasmon resonance (SPR) has been found that amplify CL signatures [12–15]. When the surface of metal is irradiated by the incident CL, the free electrons collectively oscillate at similar frequencies. The CL response can be improved through the transferring of the energy of excited CL species to metal when the CL species are in close proximity to metal [11]. This phenomenon, named metal enhanced chemiluminescence (MEC), is similar to metal-enhanced fluorescence (MEF), which describes the interactions of light emission with metal SPR. The MEC phenomenon was first discovered by using silver island films deposited onto a glass microscope slide [16]. Other metals such as gold, copper, zinc and aluminium can also be utilized. In addition to thin films, metallic nanoparticles are also employed. For example, Du et al. designed a class of gold-nanocapsule complexes which exhibited near 10-fold enhancement by coupling SPR with excitation-state molecules via non-radioactive energy transfer [17]. As a tool of CL signal amplification, MEC shows great prospects in ultrasensitive detection.

Although silver nanoparticles (AgNPs) have been widely applied in MEF-based ultrasensitive assay due to their unique optical properties, good biocompatibility and ease of chemical synthesis and modification [18], to

\* Corresponding authors.

E-mail addresses: [zongchen@cpu.edu.cn](mailto:zongchen@cpu.edu.cn) (C. Zong), [liping@cpu.edu.cn](mailto:liping@cpu.edu.cn) (P. Li).

<sup>1</sup> Contributed equally to this work.

our best knowledge, MEC assay methods based on AgNPs have not been reported. Since AgNPs show a strong SPR peak around 400 nm, which is close to the emission peak of luminol-hydrogen peroxide CL system (425 nm), excited CL species can induce/couple to the surface plasmons supported by AgNPs [11]. It follows that AgNPs have a great potential in MEC. Further, in view of that greater MEF effect has been observed when the fluorophores are simultaneously close to two nanoparticles [18,19], the hybridization between AgNPs may cause stronger MEC.

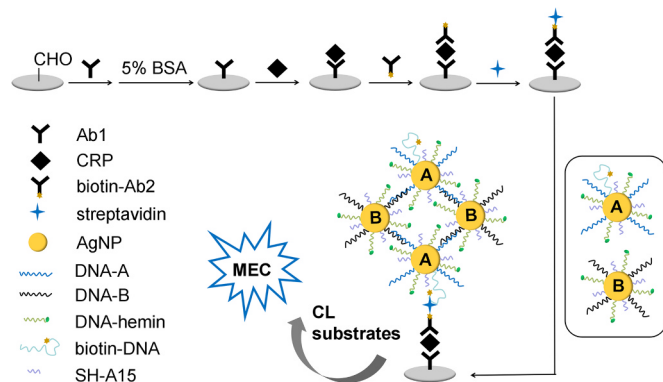
In this paper, we intended to design a novel MEC signal tag to propose an ultrasensitive immunoassay method for detection of CRP. Two kinds of AgNP probes, DNA-hemin/DNA-A/biotin-DNA modified AgNPs (Probe A) and DNA-hemin/DNA-B modified AgNPs (Probe B) were synthesized and hybridized to form AgNP hybrid probes, which brought MEC and CL signal amplification. Due to the iron (III)-protoporphyrin structure, hemin is an active cofactor of horseradish peroxidase, which is the catalyst of luminol-H<sub>2</sub>O<sub>2</sub> CL reaction. Hemin labeled ssDNA has been verified to possess higher peroxidase activity than hemin in aqueous solution [20]. With the advantage of easy modification, DNA-hemin was used in this work as a peroxidase mimic. Excited CL species around hemin molecules can couple to the surface plasmons on the surface of AgNPs. The distance between hemin molecules and AgNPs was 8 nm which was suitable for MEC. The distance between adjacent AgNPs was about 16 nm, which was controlled by the lengths of DNA. The AgNP hybrid probes were successfully applied to assay target protein CRP. A home-made immunosensor was prepared by immobilizing anti-CRP (Ab1) in the cells on an aromatic aldehyde functionalized disposable glass chip [21]. After a sandwich-type immunoassay, biotin-avidin recognition and addition of CL substrates, the AgNP hybrid probes bound on the immunosensor triggered MEC as shown in Scheme 1. CL signals were collected for different concentrations of target CRP in different cells respectively. The CL intensity of the proposed method was proportional to the logarithm value of CRP concentrations.

The proposed method showed wide linear ranges over 5 orders of magnitude and a detection limit down to 0.05 ng mL<sup>-1</sup> for detection of CRP. Moreover, it showed excellent versatility for sensitive assay of a wide range of proteins, because the presence of biotinylated DNA enabled the AgNP hybrid probes to be a universal signal tag for CL immunoassay by the specific recognition of biotin to avidin. The AgNP hybrid probes as well as the MEC-based immunoassay method could be suitable for ultrasensitive and accurate analysis of protein markers, showing great potentials in early clinical diagnosis of cerebrovascular disease.

## 2. Experimental part

### 2.1. Reagents and apparatus

Glass chips modified with aromatic aldehyde group were purchased from Shanghai BaiO Technology Co., Ltd. (China). The Ab1 and



**Scheme 1.** Schematic diagram of procedure of MEC immunoassay for detection of CRP based on AgNP hybrid probes.

detection antibodies (Ab2) of CRP (mouse monoclonal antibodies, ab136176 and ab8278) were from Abcam Trading Co., Ltd. (Shanghai). CRP antigen (PC04N991) and CL substrates (luminol-*p*-iodophenol and H<sub>2</sub>O<sub>2</sub>) were both from Beijing KeyBiotech Co., Ltd. (China). Human myoglobin (Mb) and MB isoenzyme of creatine kinase (CKMB) were obtained from Beijing Biosynthesis Biotechnology Co., Ltd. (China). The Ab2 of CRP was modified with biotin to form biotin-Ab2 and purified by Beijing Biosynthesis Biotechnology Co., Ltd. (China). All of the oligonucleotides were synthesized by Shanghai Sangon Biotechnology Co., Ltd. (China). The oligonucleotides were derived with alkyl thiol group at the 5' terminus and their sequences are shown in [Support materials Table S1](#). Streptavidin was purchased from Promega (USA). Tween-20 was purchased from Sigma-Aldrich (USA). Bovine serum albumin (BSA) was purchased from Biosharp Co., Ltd. (China). 40 nm AgNPs were purchased from Shanghai So-Fe Biomedicine Co., Ltd. (China).

Silver nitrate, sodium borohydride and trisodium citrate were used to synthesize colloidal AgNPs. Phosphate-buffered saline (PBS, 0.01 M, pH 7.4) was prepared by mixing the stock solutions of NaCl, KCl, KH<sub>2</sub>PO<sub>4</sub> and Na<sub>2</sub>HPO<sub>4</sub>·12H<sub>2</sub>O and used as coupling buffer for the immobilization of Ab1. 0.05% Tween-20 was spiked into 0.01 M PBS as the washing buffer. Blocking buffer, which was used to block the residual reactive sites on the immunosensor chip, was 0.01 M PBS containing 5% BSA. 0.2 M PBS<sup>+</sup> was 0.001 M PBS containing 0.2 M NaCl and 1 mM MgCl<sub>2</sub>. Ultrapure water from a Milli-Q water purification system (≥18 MΩ cm, Millipore, Milford, MA, USA) was used in the whole assay. Clinical serum samples were from Jiangsu Province Hospital of Traditional Chinese Medicine. All other reagents were of analytical grade and used as received.

The ultraviolet-visible (UV–vis) absorption spectra were recorded with a micro spectrophotometer (Nano-100, Hangzhou Allsheng Instruments Co., Ltd.). CL signals were collected by an IFFM-E luminescent analyzer (Xi'an Remax Analysis Instruments Co., Ltd., China). A JEM-200CX transmission electron microscope (TEM) (JEOL Ltd., Tokyo, Japan) was used to characterize the AgNPs, Probe A, Probe B and Probe AB formed by Probe A and Probe B reacting for 60 min in solution at room temperature (RT). Scanning electron micrographs of immunosensor chip before/after modification were obtained with an S-3400N II scanning electron microscope (SEM) (JEOL Ltd., Tokyo, Japan). The control levels of the CRP in clinical serum samples were obtained with Beckman Immage800 Immunochemistry System (Beckman Coulter, Inc., USA). Atomic absorption spectroscopy (AAS) (Model 180–80, Hitachi Co., Japan) was used to obtain the actual concentration of silver atoms in the final AgNPs solution.

### 2.2. Fabrication of immunosensor chip

A layer of photo-inactive film with 48 cells (4 mm diameter, 1 mm edge-to-edge separation) in a 4 × 12 format was fixed on the aldehyde modified glass chip manually [21]. The thickness of the film was ~0.1 mm and the maximum sample volumes required in each cell was 10 μL. Then, 10 μL Ab1 of CRP at 10 μg mL<sup>-1</sup> was dropped in each cell and incubated overnight at 4 °C. The antibody immobilization can be achieved efficiently through the interaction between amino group of antibody and aromatic aldehydes on the chip. After washing and drying, 10 μL of blocking buffer was dropped into each cell for 2 h to block the unreacted aldehyde group. After washing and drying, the immunosensor chip was obtained and stored at 4 °C before use.

### 2.3. Synthesis of AgNPs

The AgNPs were synthesized according to conventional methods by using NaBH<sub>4</sub> reduction of AgNO<sub>3</sub> in the presence of trisodium citrate [22]. Briefly, 10 mL of 1.0 mM silver nitrate solution was added dropwise to a chilled-solution mixture of sodium borohydride (2.0 mM, 30 mL) and trisodium citrate (34 mM, 2 mL) under vigorous stirring condition at RT. Sodium borohydride and trisodium citrate were used

as the reducing and stabilizing agent respectively. The colorless solution turned light yellow initially, but then turned a brighter yellow when all silver nitrate was added, which indicated that AgNPs had been successfully prepared. The entire addition took approximately 3 min, and stirring of the solution continued for further 30 min to complete the reaction. The as-prepared AgNPs solution was stored at 4 °C before use.

#### 2.4. Preparation of Probe A

Probe A was prepared according to the literature with some modification [18]. In brief, 25  $\mu\text{L}$  of 10  $\mu\text{M}$  DNA-A, 25  $\mu\text{L}$  of 10  $\mu\text{M}$  DNA-hemin and 25  $\mu\text{L}$  of 10  $\mu\text{M}$  biotin-DNA were added slowly into 1 mL of the colloidal silver solution respectively to react at RT under gentle stirring. After incubation for 18 h, 25  $\mu\text{L}$  of 10  $\mu\text{M}$  blocking SH-A15 was added to the solution with stirring for 2 h to passivate the left active sites on AgNPs. Subsequently, 122  $\mu\text{L}$  of 0.01 M PBS (pH 7.4) was added to the solution and reacted for 6 h. Then 21  $\mu\text{L}$  of 2 M NaCl was added to the solution and this step was repeated after a 3 h interval. A 26  $\mu\text{L}$  of 2 M NaCl was then added to the solution after 12 h and this step was repeated after a 3 h interval. After 48 h, the resulting solution was purified by centrifugation at 15,000 rpm at 14 °C for 15 min and the precipitates were dispersed in 1 mL of 0.2 M PBS<sup>+</sup>. By taking advantage of slight modification and the very gentle and gradual increase of NaCl concentration, AgNPs functionalized by polyadenine (A) can withstand at least a 300 mM NaCl concentration with excellent optical property [18,23].

#### 2.5. Preparation of Probe B

Probe B was prepared according to the literature with some modification [18]. In brief, 25  $\mu\text{L}$  of 10  $\mu\text{M}$  DNA-B and 25  $\mu\text{L}$  of 10  $\mu\text{M}$  DNA-hemin were added slowly into 1 mL of the colloidal silver solution respectively to react for 18 h at RT under gentle stirring. The rest of steps were the same as above.

#### 2.6. Preparation of controlled tag (Probe C)

Probe C was prepared according to the literature with some modification [18]. In brief, 25  $\mu\text{L}$  of 10  $\mu\text{M}$  DNA-B was added slowly into 1 mL of the colloidal silver solution respectively to react for 18 h at RT under gentle stirring. The rest of steps were the same as above.

#### 2.7. MEC immunoassay strategy

The procedure of proposed MEC immunoassay method is demonstrated in Scheme 1. To obtain the calibration curve of CRP, 8  $\mu\text{L}$  of the standard solutions diluted with 0.01 M PBS (pH 7.4) to different concentrations were added to different sensing sites and incubated for 15 min. After washing and drying, 8  $\mu\text{L}$  of biotin-Ab2 was added and incubated for 15 min as well, followed by washing and drying. Then 8  $\mu\text{L}$  of streptavidin was added to bind to biotin-Ab2 and incubated for

another 15 min. After washing and drying, 4  $\mu\text{L}$  of Probe A and 4  $\mu\text{L}$  of Probe B respectively were added and incubated for 60 min, followed by washing and drying. Finally, 8  $\mu\text{L}$  of CL substrates were delivered into the sensing cells to trigger the CL reaction. In order to perform the detection of CRP in clinical serum samples, 8  $\mu\text{L}$  of serum sample was added to the sensing cells to perform the same procedures.

### 3. Results and discussion

#### 3.1. Characterization of AgNPs

The appearance and size of the prepared AgNPs were observed by TEM. The AgNPs are spherical with an average particle size of about 10 nm (See the Support materials Fig. S1A) and the UV–vis spectrum of AgNPs shows an absorption peak at 391 nm (See the Support materials Fig. S1B), which is approximately identical to the literature [22].

The number of Ag atoms in each AgNP and number of AgNPs are calculated to be 17,453 and  $6.70 \times 10^{12}$  NPs/mL [24] (See the Support materials (S1)). Measured by AAS (See the Support materials Fig. S2), the actual concentration of Ag in the final AgNPs solution is 0.195 mM. The concentration of AgNPs is calculated to be 11.2 nM.

#### 3.2. Characterization of immunosensor chip

The glass chip modified with aldehyde groups shows a smooth and homogeneous surface (See the Support materials Fig. S3A). While Ab1 was immobilized due to the interaction with aldehyde groups, a distinct aggregation of the trapped biomolecules on the surface can be observed (See the Support materials Fig. S3B), indicating successful assembly of Ab1 on the sensing sites [25].

#### 3.3. Characterization of Probe A, Probe B and Probe AB

The appearance and size of the prepared Probe A, Probe B and Probe AB were all observed by TEM. As shown in Fig. 1, Probe A (Fig. 1A) and Probe B (Fig. 1B) have the similar morphology and size. Most of them are spherical. Probe AB, which is formed by Probe A and Probe B reacting for 60 min in solution at RT, is vastly different from individual Probe A and Probe B in size and morphology. The size of Probe AB (Fig. 1C) is approximately 325 nm and its morphology resembles an aggregated.

Additionally, UV–vis spectra were used to characterize Probe A, Probe B and Probe AB. Probe A (Fig. 2A, black line) and Probe B (Fig. 2A, red line) both have an absorption peak at 398 nm and almost the same absorbance. Compared with AgNPs, they show a red shift of 7 nm and have lower absorbance respectively, implying the successful modification of DNA strands on the surface of AgNPs.

On the basis of the absorbance of AgNPs (See the Support materials Fig. S1B), Probe A and Probe B (Fig. 2A), the concentration of Probe A and Probe B can be calculated as 3.11 nM and 3.04 nM respectively. Since Probe A and Probe B are completely similar in properties, Probe A

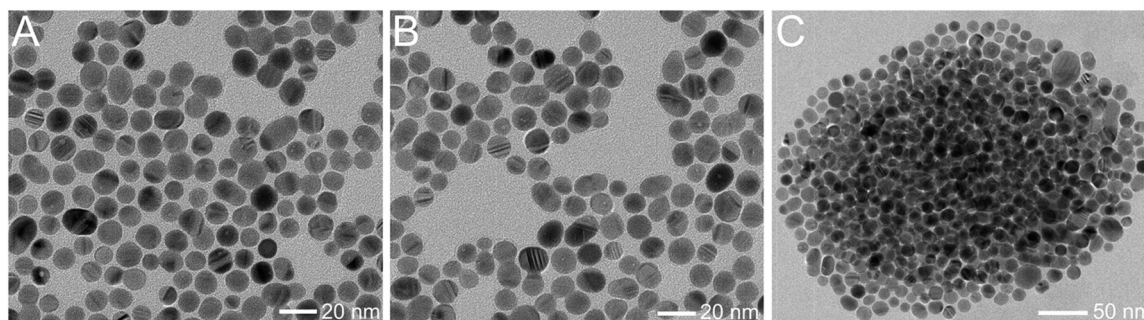
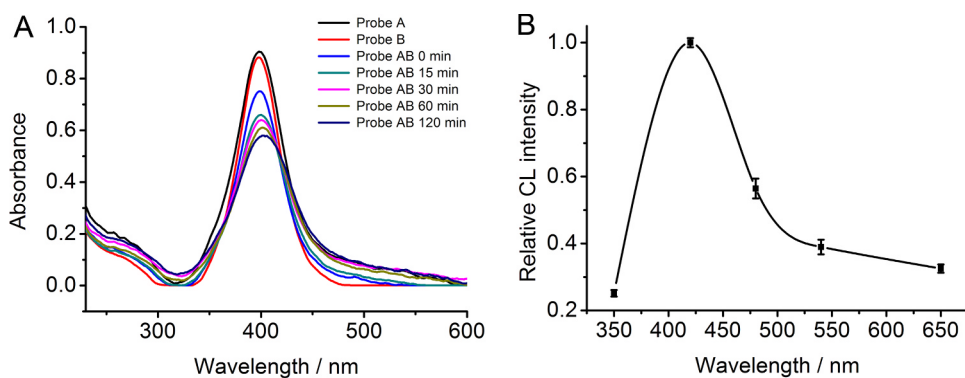
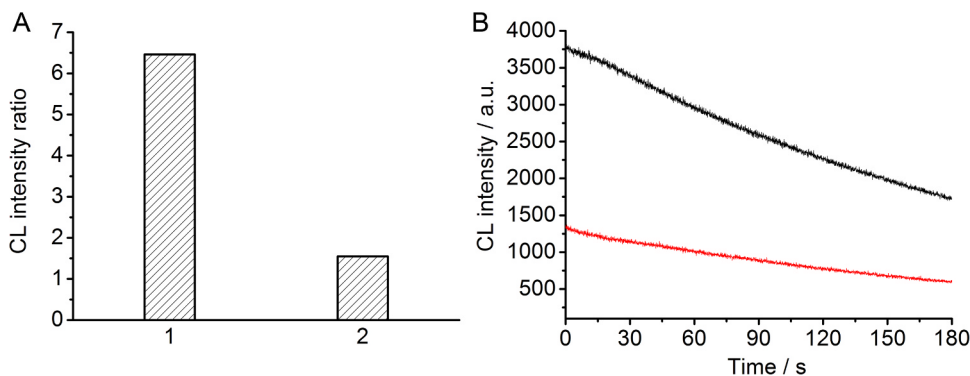


Fig. 1. TEM images of Probe A (A), Probe B (B) and Probe AB formed by Probe A and Probe B reacting for 60 min in solution at RT (C).



**Fig. 2.** (A) UV-vis spectra of Probe A, Probe B and Probe AB formed by Probe A and Probe B with different reacting time in solution at RT. (B) CL spectra of DNA-hemin using luminol-*p*-iodophenol and H<sub>2</sub>O<sub>2</sub> CL system. Number of references is 3. (For interpretation of the references to color in this figure, the reader is referred to the web version of this article)



**Fig. 3.** (A) (1) CL intensity ratio of Probe AB and Probe AA ( $CL_{[Probe A + Probe B]} / CL_{[Probe A + Probe A]}$ ); (2) CL intensity ratio of Probe AC and Probe AA ( $CL_{[Probe A + Probe C]} / CL_{[Probe A + Probe A]}$ ). (B) Kinetic curve of the luminol-*p*-iodophenol-H<sub>2</sub>O<sub>2</sub> CL reaction catalyzed by Probe AB (black line) and Probe AA (red line) captured on the immunosensor chip. (CRP: 0.03 mg mL<sup>-1</sup>). (For interpretation of the references to color in this figure, the reader is referred to the web version of this article)

is chosen as the detection probe in the following experiments.

By comparing the CL signal catalyzed by Probe A and free DNA-hemin under the same CL catalytic conditions, the concentration of active DNA-hemin in Probe A is estimated to be 32.15 nM. While the concentration of Probe A is 3.11 nM, the number of active DNA-hemin units on per Probe A is estimated to be 10, which indicates 10 signal molecules for a single probe, leading to the signal amplification (See the [Support materials \(S2\)](#)).

### 3.4. MEC of the Probe AB

As shown in [Fig. S4](#), Probe A containing DNA-hemin (18 A/30 A/36 A) exhibits lower CL intensities than Probe A containing DNA-hemin (24A). The best distance between each AgNP and DNA-hemin are verified to be 8 nm for achieving MEC effect, in corresponding with the previous observations with MEF [26].

The size of the AgNPs also poses a significant influence on the CL enhancement. Compared with the 10 nm AgNPs, home-made 6 nm AgNPs [21] result in much lower CL intensification ([Fig. S5](#)), consistent with the previous observations with MEC [17]. Considering AgNPs with bigger size brought steric modification, poor stability and dispersivity, 10 nm AgNPs were chosen for the AgNPs-based analytical methods.

With the increasing hybridization time of Probe A and Probe B ([Fig. 2A](#), from 0 to 120 min), the absorbance of Probe AB gets gradual broadening and shows apparent red shift of 5 nm (from 398 nm to 403 nm). The absorbance of Probe AB at 398 nm decreases, demonstrating that more and more Probe A and Probe B hybridized with each other to form Probe AB ([Fig. 2A](#)). The absorbance of Probe AB at 425 nm increases, which is corresponded to the maximum emission wavelength of DNA-hemin using luminol-*p*-iodophenol and H<sub>2</sub>O<sub>2</sub> CL system ([Fig. 2B](#)). The red shift and broadening of the SPR peak of Probe AB can provide a better overlap with the maximum emission wavelength of DNA-hemin catalyzed CL, thus resulting in greater MEC.

As verified in [Fig. 3A](#), the CL intensity ratio of Probe AB in the homogenous solution is 6.5 ( $CL_{[Probe A + Probe B]} / CL_{[Probe A + Probe A]} = 6.5$ ), which is higher than Probe A and Probe C ( $CL_{[Probe A + Probe C]} /$

$CL_{[Probe A + Probe A]} = 1.5$ ). These results suggest that the hybridization of Probe A and Probe B can bring combined CL enhancement of MEC and increase in hemin content, while the hybridization of Probe A and Probe C only gives rise to CL enhancement of MEC. Hence, it can be concluded that MEC of Probe AB and increase of hemin content are both responsible for amplified CL signal.

Kinetic curves of the CL reaction catalyzed by Probe AA (Probe A + Probe A) ([Fig. 3B](#), red line) and Probe AB ([Fig. 3B](#), black line) bound to the sandwich immunocomplex were studied with a static method. The CL reaction occurred immediately upon the addition of CL substrates, while the CL depletion of Probe AB was faster than Probe AA. The higher rate can be described by two explanations: (1) reduced excited state lifetime of the CL species due to metal SPR, (2) increased hemin content, with higher catalysis of the CL reaction [11].

### 3.5. Optimization of hybridization time

For convenient operation, the incubation steps of immunoassay were performed at RT. 0.003 mg mL<sup>-1</sup> CRP was used to explore the effect of hybridization time of Probe A and Probe B on the CL enhancement of Probe AB. As shown in [Fig. 4A](#), with the incubation time increasing, the CL intensity of signal and noise both increase. However, the signal has more significant growth than the noise and the signal-to-noise ratio (S/N) reaches the maximum value at 60 min. Therefore, 60 min is selected as the optimal hybridization time for the immunoassay.

To further prove that Probe AB brings the CL enhancement, Probe AB, Probe A and free DNA-hemin assisted by biotin-24T were utilized to compare CL intensity ([Fig. 4B](#)). The CL intensity ratio of Probe AB to DNA-hemin ( $CL_{[Probe A + Probe B]} / CL_{[DNA-hemin]}$ ) increases from 14 to 25 with the incubation time increasing (from 15 to 90 min), while the CL intensity ratio of Probe AA to DNA-hemin ( $CL_{[Probe A + Probe A]} / CL_{[DNA-hemin]}$ ) almost maintains about 9.

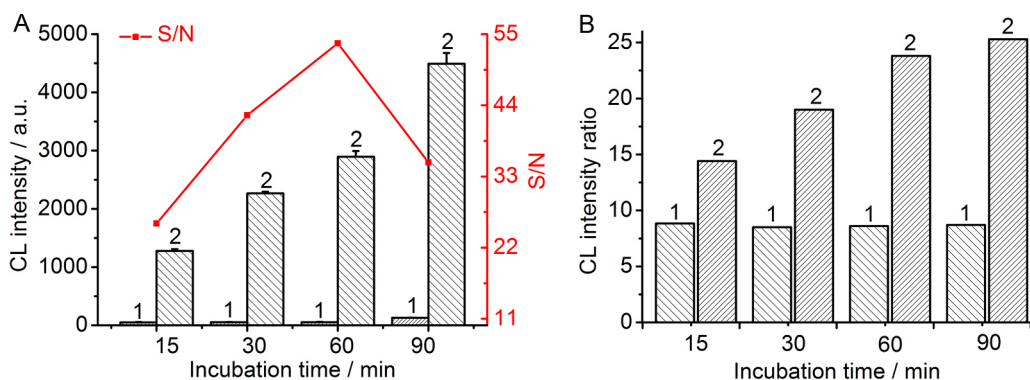


Fig. 4. The optimization of incubation time for detection of CRP at  $0.003 \text{ mg mL}^{-1}$ . (A) (1) The CL intensity of noise; (2) The CL intensity of signal. The red line chart is the relationship of S/N and incubation time. (B) The relationship of CL intensity ratio and incubation time. (1)  $\text{CL}_{[\text{Probe A} + \text{Probe B}]} / \text{CL}_{[\text{DNA-hemin}]}$ ; (2)  $\text{CL}_{[\text{Probe A} + \text{Probe A}]} / \text{CL}_{[\text{DNA-hemin}]}$ . Number of experiments is 3. (For interpretation of the references to color in this figure legend, the reader is referred to the web version of this article)

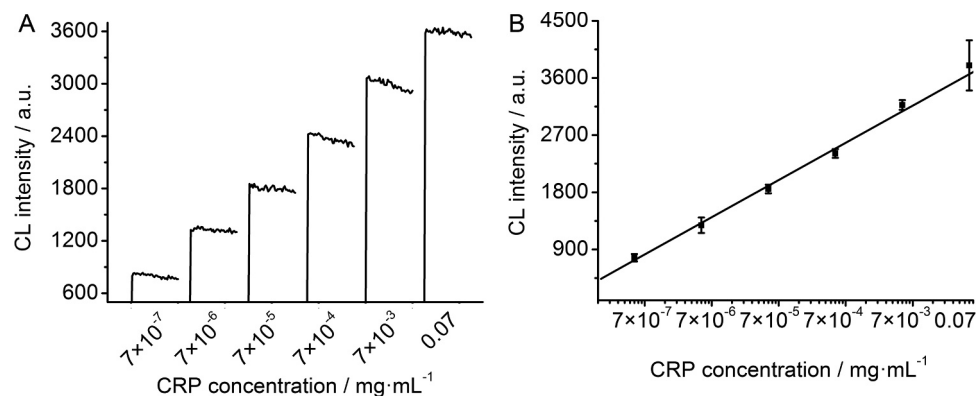


Fig. 5. (A) CL response to CRP at  $7 \times 10^{-7}$ ,  $7 \times 10^{-6}$ ,  $7 \times 10^{-5}$ ,  $7 \times 10^{-4}$ ,  $7 \times 10^{-3}$  and  $0.07 \text{ mg mL}^{-1}$ . (B) Calibration curve for immunoassay of CRP. Number of experiments is 3.

### 3.6. MEC immunoassay for detection of CRP

The MEC immunoassay of CRP was carried out under the optimal experimental conditions. The CL intensity increases linearly with the increasing logarithm of CRP concentration (Fig. 5A), leading to a wide detection range of 5 orders of magnitude (from  $7 \times 10^{-7}$  to  $0.07 \text{ mg mL}^{-1}$ ) with a correlation coefficient of 0.9945 (Fig. 5B). The limit of detection is estimated to be  $0.05 \text{ ng mL}^{-1}$  ( $\sim 0.43 \text{ pM}$ ) corresponding to the signal of 3 SD. The low detection limit and wide detection range are comparable to the sensitive CL immunoassay methods [2,6,27–31] based on other amplification strategies (See the Support materials Table S2). The prepared Probe A and Probe B are stored in the dark at  $4^\circ\text{C}$ . After two-weeks storage, the CL signal remains at 93% of the initial response, exhibiting good stability.

### 3.7. Evaluation of cross-reactivity

The cross-reactivity between CRP immunosensor chip and non-specific analytes was evaluated by comparing the CL intensity after incubation the chip with blank solution; the mixture solution of  $7 \times 10^{-5} \text{ mg mL}^{-1}$  CKMB and  $7 \times 10^{-5} \text{ mg mL}^{-1}$  Mb;  $7 \times 10^{-5} \text{ mg mL}^{-1}$  CRP; and the mixture solution of  $7 \times 10^{-5} \text{ mg mL}^{-1}$  CKMB,  $7 \times 10^{-5} \text{ mg mL}^{-1}$  Mb and  $7 \times 10^{-5} \text{ mg mL}^{-1}$  target CRP. As expected, the CRP immunosensor chip shows obvious responses to target CRP and the mixture containing target antigen (See the Support materials Fig. S6), indicating good specificity and negligible nonspecific binding.

### 3.8. Detection of CRP in clinical serum samples

To evaluate the analytical reliability and application potential of the proposed MEC immunoassay method, different concentrations of CRP

in human serum samples were tested. The assay results obtained by the proposed method were compared with the reference values obtained by commercial specific protein analyzer. The results with relative errors less than 4.94% for the detection of CRP (See the Support materials Table S3) are acceptable, indicating the practicability of the proposed method and the Probe AB.

## 4. Conclusions

This work proposes a highly sensitive metal-enhanced CL immunoassay for detection of CRP based on AgNP hybrid probes. By loading multiple DNA-hemin on the surface of AgNPs and strictly controlling the distance between each AgNP and DNA-hemin, MEC effect and CL signal amplification can be achieved. With the use of two kinds of AgNPs modified by complementary oligonucleotides, DNA-hemin can be simultaneously fixed close to two AgNPs along with the hybridization between AgNPs, leading to greater MEC and signal amplification. The protocol shows a wide detection range and a detection limit down to  $0.05 \text{ ng mL}^{-1}$ . This method is also available to measure analytes in clinical serum samples with good accuracy, high sensitivity, low cost, small consumption and convenient operation. In a word, the MEC immunoassay method as well as AgNP hybrid probes provides great potentials in early clinical diagnosis of cerebrovascular disease and shows a good perspective for application of competitive immunoassay for small molecules detection.

## Acknowledgements

This work is supported by the National Natural Science Foundation of China (21505160, 81730104), Natural Science Foundation of Jiangsu Province (BK20150690) and 111 Project (no. B16046).

## Appendix A. Supporting information

Supplementary data associated with this article can be found in the online version at [doi:10.1016/j.talanta.2019.02.060](https://doi.org/10.1016/j.talanta.2019.02.060).

## References

- [1] M. Di Napoli, M.S. Elkind, D.A. Godoy, P. Singh, F. Papa, A. Popa-Wagner, Role of C-reactive protein in cerebrovascular disease: a critical review, *Expert Rev. Cardiovasc. Ther.* 9 (2011) 1565–1584, <https://doi.org/10.1586/ERC.11.159>.
- [2] Y. Xing, Q. Gao, Y.M. Zhang, L. Ma, K.Y. Loh, M.L. Peng, C. Chen, Y.L. Cui, The improved sensitive detection of C-reactive protein based on the chemiluminescence immunoassay by employing monodispersed PAA-Au/Fe<sub>3</sub>O<sub>4</sub> nanoparticles and zwitterionic glycerophosphoryl choline, *J. Mater. Chem. B* 5 (2017) 3919–3926, <https://doi.org/10.1039/C7TB00637C>.
- [3] S.W. Shan, Z.Y. He, S.F. Mao, M.S. Jie, L.L. Yi, J.M. Lin, Quantitative determination of VEGF165 in cell culture medium by aptamer sandwich based chemiluminescence assay, *Talanta* 171 (2017) 197–203, <https://doi.org/10.1016/j.talanta.2017.04.057>.
- [4] A. Tiwari, S.J. Dhoble, Recent advances and developments on integrating nanotechnology with chemiluminescence assays, *Talanta* 180 (2018) 1–11, <https://doi.org/10.1016/j.talanta.2017.12.031>.
- [5] Y.L. Sun, Y.H. Wang, J.B. Li, C.F. Ding, Y.N. Lin, W.Y. Sun, C.N. Luo, An ultra-sensitive chemiluminescence aptasensor for thrombin detection based on iron porphyrin catalyzing luminescence desorbed from chitosan modified magnetic oxide graphene composite, *Talanta* 174 (2017) 809–818, <https://doi.org/10.1016/j.talanta.2017.07.001>.
- [6] J.W. Liu, Z.J. Zhao, S.T. Li, L.L. Zhang, Y. Huang, S.L. Zhao, A novel microchip electrophoresis-based chemiluminescence immunoassay for the detection of alpha-fetoprotein in human serum, *Talanta* 165 (2017) 107–111, <https://doi.org/10.1016/j.talanta.2016.12.038>.
- [7] J. Li, X.H. Li, Y. Huang, Y.H. Zhong, Q.C. Lan, X.Y. Wu, R.X. Hu, G.S. Zhang, X.Y. Hua, Z.J. Yang, Biofunctionalized mesoporous silica nanospheres for the ultra-sensitive chemiluminescence immunoassay of tumor markers, *New J. Chem.* 42 (2018) 11264–11267, <https://doi.org/10.1039/C8NJ02203H>.
- [8] Z.J. Yang, M.M. Lu, J. Li, Z.N. Tan, H. Dai, X.A. Jiao, X.Y. Hu, Nitrogen-doped graphene-chitosan matrix based efficient chemiluminescent immunosensor for detection of chicken interleukin-4, *Biosens. Bioelectron.* 89 (2017) 558–564, <https://doi.org/10.1016/j.bios.2016.02.046>.
- [9] S. Gnaima, A. Scomarino, S. Dasa, R. Blaub, R. Satchi-Fainarob, D. Shabata, Real-time monitoring of prodrug activation by direct-mode of chemiluminescence, *Angew. Chem. Int. Ed.* 57 (2018) 9033–9037, <https://doi.org/10.1002/anie.201804816>.
- [10] W.W. Wang, X.X. Su, H. Ouyang, L. Wang, Z.F. Fu, A novel immunochromatographic assay based on a time-resolved chemiluminescence strategy for the multiplexed detection of ractopamine and clenbuterol, *Anal. Chim. Acta* 917 (2016) 79–84, <https://doi.org/10.1016/j.aca.2016.03.001>.
- [11] K. Aslan, C.D. Geddes, Metal-enhanced chemiluminescence: advanced chemiluminescence concepts for the 21st century, *Chem. Soc. Rev.* 40 (46) (2009) 2556–2564, <https://doi.org/10.1039/b807498b>.
- [12] H. Chen, R. Li, H. Li, J.M. Lin, Plasmon-assisted enhancement of the ultraweak chemiluminescence using Cu/Ni metal nanoparticles, *J. Phys. Chem. C* 116 (28) (2012) 14796–14803, <https://doi.org/10.1021/jp303092d>.
- [13] H. Chen, L. Lin, H. Li, J. Li, J.M. Lin, Aggregation-induced structure transition of protein-stabilized zinc/copper nanoclusters for amplified chemiluminescence, *ACS Nano* 9 (2) (2015) 2173–2183, <https://doi.org/10.1021/acsnano.5b00141>.
- [14] M. Iranifam, Chemiluminescence reactions enhanced by silver nanoparticles and silver alloy nanoparticles: applications in analytical chemistry, *Trac-Trend Anal. Chem.* 82 (2016) 126–142, <https://doi.org/10.1016/j.trac.2016.05.018>.
- [15] S.Q. Lie, D.M. Wang, M.X. Gao, C.Z. Huang, Controllable copper deficiency in Cu<sub>2–x</sub>Se nanocrystals with tunable localized surface plasmon resonance and enhanced chemiluminescence, *Nanoscale* 6 (17) (2014) 10289–10296, <https://doi.org/10.1039/C4NR02294G>.
- [16] M.H. Chowdhury, K. Aslan, S.N. Malyn, J.R. Lakowicz, C.D. Geddes, Metal-enhanced chemiluminescence, *J. Fluoresc.* 16 (3) (2006) 295–299, <https://doi.org/10.1007/s10895-006-0082-z>.
- [17] J.J. Du, J. Jin, Y. Liu, J. Li, T. Tokatlian, Z.H. Lu, T. Segura, X.B. Yuan, X.J. Yang, Y.F. Lu, Gold-nanocrystal-enhanced bioluminescent nanocapsules, *ACS Nano* 8 (10) (2014) 9964–9969, <https://doi.org/10.1021/nn504371h>.
- [18] H. Li, W.B. Qiang, M. Vuki, D.K. Xu, H.Y. Chen, Fluorescence enhancement of silver nanoparticle hybrid probes and ultrasensitive detection of IgE, *Anal. Chem.* 83 (23) (2011) 8945–8952, <https://doi.org/10.1021/ac201574s>.
- [19] J. Zhang, Y. Fu, M.H. Chowdhury, J.R. Lakowicz, Metal-enhanced single-molecule fluorescence on silver particle monomer and dimer: coupling effect between metal particles, *Nano Lett.* 7 (7) (2007) 2101–2107, <https://doi.org/10.1021/nl071084d>.
- [20] Q.B. Wang, N. Xu, J.P. Lei, H.X. Ju, Regulative peroxidase activity of DNA-linked hemin by graphene oxide for fluorescence DNA Sensing, *Chem. Commun.* 50 (2014) 6714–6717, <https://doi.org/10.1039/c4cc02273d>.
- [21] C. Zong, D.D. Zhang, H. Yang, S.M. Wang, M. Chu, P. Li, Chemiluminescence immunoassay for cardiac troponin T by using silver nanoparticles functionalized with hemin/G-quadruplex DNzyme on a glass chip array, *Microchim. Acta* 184 (2017) 3197–3204, <https://doi.org/10.1007/s00604-017-2331-z>.
- [22] R. Choudhury, A. Purkayastha, D. Debnath, T.K. Misra, Recognition of silver nanoparticles surface-adsorbed citrate anions by macrocyclic polyammonium cations: a spectrophotometric approach to study aggregation kinetics and evaluation of association constant, *J. Mol. Recognit.* 29 (9) (2016) 452–461, <https://doi.org/10.1002/jmr.2544>.
- [23] I. Tokareva, E. Hutter, Hybridization of oligonucleotide-modified silver and gold nanoparticles in aqueous dispersions and on gold films, *J. Am. Chem. Soc.* 126 (2004) 15784–15789, <https://doi.org/10.1021/ja046779k>.
- [24] R. Meelapsom, P. Jarujamrus, M. Amatatongchai, S. Chairam, C. Kulsing, W. Shen, Chromatic analysis by monitoring unmodified silver nanoparticles reduction on double layer microfluidic paper-based analytical devices for selective and sensitive determination of mercury(II), *Talanta* 155 (2016) 193–201, <https://doi.org/10.1016/j.talanta.2016.04.037>.
- [25] Z.J. Yang, H. Liu, C. Zong, F. Yan, H.X. Ju, Automated support resolution strategy for a one-way chemiluminescent multiplex immunoassay, *Anal. Chem.* 81 (2009) 5484–5489, <https://doi.org/10.1021/ac900724m>.
- [26] Y. Wang, Z.H. Li, H. Li, M. Vukib, D.K. Xu, H.Y. Chen, A novel aptasensor based on silver nanoparticle enhanced fluorescence, *Biosens. Bioelectron.* 32 (2012) 76–81, <https://doi.org/10.1016/j.bios.2011.11.030>.
- [27] B.F. Hu, J.J. Li, L. Mou, Y. Liu, J.Q. Deng, W. Qian, J.S. Sun, R.T. Cha, X.Y. Jiang, An automated and portable microfluidic chemiluminescence immunoassay for quantitative detection of biomarkers, *Lab Chip* 17 (2017) 2225–2234, <https://doi.org/10.1039/c7lc00249a>.
- [28] J. Li, J.J. Zhao, S.T. Li, L.L. Zhang, C.Q. Lan, Y. Huang, S.L. Zhao, A novel dual targets simultaneous chemiluminescence signal amplification strategy for enhancing the sensitivity of multiple biomolecules detection, *Anal. Methods* 9 (2017) 6785–6790, <https://doi.org/10.1039/C7AY02102J>.
- [29] J.M. Wang, S.F. Mao, H.F. Li, J.M. Lin, Multi-DNAzymes-functionalized gold nanoparticles for ultrasensitive chemiluminescence detection of thrombin on microchip, *Anal. Chim. Acta* 1027 (2018) 76–82, <https://doi.org/10.1016/j.aca.2018.04.028>.
- [30] P. Zou, Y.L. Liu, H.Y. Wang, J. Wu, F.F. Zhu, H. Wu, G-quadruplex DNzyme-based chemiluminescence biosensing platform based on dual signal amplification for label-free and sensitive detection of protein, *Biosens. Bioelectron.* 79 (2016) 29–33, <https://doi.org/10.1016/j.bios.2015.12.012>.
- [31] L. Ma, Y.Y. Sun, X.J. Kang, Y.K. Wan, Development of nanobody-based flow injection chemiluminescence immunoassay for sensitive detection of human prealbumin, *Biosens. Bioelectron.* 61 (2014) 165–171, <https://doi.org/10.1016/j.bios.2014.04.026>.